MAJOR ARTICLE

Lack of Galectin-3 Prevents Cardiac Fibrosis and Effective Immune Responses in a Murine Model of *Trypanosoma cruzi* Infection

Miguel A. Pineda,[a] Henar Cuervo,[a] Manuel Fresno, Manuel Soto, and Pedro Bonay

Centro de Biología Molecular Severo Ochoa, Nicolás Cabrera 1, Universidad Autónoma de Madrid, Spain

Background. Chagas disease is caused by the protozoan *Trypanosoma cruzi,* affecting millions of people worldwide. One of the major causes of mortality in the disease is the cardiomyopathy observed in chronic patients, despite the low number of parasites detected in cardiac tissue. Galectin-3, a carbohydrate-binding protein with affinity for β-galactoside–containing glycoconjugates, is upregulated upon infection, and it has been recently involved in the pathophysiology of heart failure.

Methods. We investigated the role of galectin-3 in systemic and local responses in a murine model of *T. cruzi* infection, using knockout animals. Molecular mechanisms underlying galectin-3–dependent inflammatory responses were further assessed in cultured dendritic cells in vitro.

Results. Mice deficient for galectin-3 have elevated blood parasitemia levels and impaired cytokine production during infection. Remarkably, galectin-3 promotes cellular infiltration in the heart of infected mice and subsequent collagen deposition and cardiac fibrosis. Furthermore, we show that an unbalanced Toll-like receptor expression on antigen-presenting cells may be the cause of the impaired immune response observed in galectin-3–deficient mice in vivo.

Conclusions. These results suggest that galectin-3 is strongly involved in Chagas disease, not only in the immune response against *T. cruzi*, but also in mediating cardiac tissue damage.

Keywords. *Trypanosoma cruzi*; galectin-3; cardiac fibrosis; Toll-like receptor; inflammation; innate immunity.

Chagas disease is a chronic illness caused by the protozoan *Trypanosoma cruzi*. It presents a short acute phase characterized by detectable parasitemia with mild and unspecific symptoms. Later, parasitemia becomes virtually undetectable, and patients enter a symptomless phase that can last for decades. One third of these individuals will develop clinical manifestations, such as chronic chagasic cardiomyopathy (CCC) [1]. Despite chronic tissue damage, the scarcity of parasites in histological sections from patients and the presence of autoreactive responses have raised 2 primary hypotheses to account for pathogenesis. First, the pathology is directly linked to parasite persistence in infected tissues [2, 3], and second, the pathogenesis has an autoimmune basis [4–6] in which the parasite induces immune responses targeted at self tissues, although it is likely that both occur simultaneously [7, 8]. Indeed, clinical manifestations at chronic stages depend largely on early parasite-host interactions and the subsequent activation of innate immunity. Therefore, the study of molecules involved in host-parasite interaction leading to production of inflammatory mediators and tissue damage appears to be key to understanding molecular mechanisms associated with CCC. Toll-like receptors (TLRs) are known to recognize *T. cruzi* [9, 10] and induce T-helper type 1 (Th1)/Th2 responses [11–14], along with expression of regulatory interleukin 10 (IL-10), which inhibits interferon γ (IFN-γ)–mediated parasite killing [15]. Accordingly, immune mechanisms

Received 9 November 2014; accepted 16 March 2015; electronically published 24 March 2015.

[a]Present affiliations: Institute of Infection, Immunity, and Inflammation, University of Glasgow, United Kingdom (M. A. P.); and Irving Cancer Research Center, New York, New York (H. C.).

Correspondence: Miguel A. Pineda, PhD, University of Glasgow, UK (miguel.pineda@glasgow.ac.uk).

The Journal of Infectious Diseases® 2015;212:1160–71

DOI: 10.1093/infdis/jiv185

fail to eliminate parasites and eventually lead to a polyclonal expansion of lymphocytes, generating local inflammation and recruitment of lymphocytes and macrophages to cardiac tissue that perpetuate chronic damage.

Galectins are defined by a conserved carbohydrate recognition domain with an affinity for β-galactosides [16]. Among them, galectin-3 (gal-3) is a strong proinflammatory mediator that also appears to recognize glycans present in a number of pathogens [17, 18]. Importantly, gal-3 is upregulated after *T. cruzi* infection in dendritic cells (DCs) and B cells [19, 20], suggesting a potential role for this protein in Chagas immunopathology, since many parasite products are highly glycosylated [14, 21, 22]. Yet, despite the proinflammatory nature of gal-3 and its role in parasite adhesion to host cells [23, 24], the relevance of this protein in the immune response against *T. cruzi* and subsequent CCC development remains undetermined. Here we show that gal-3 knock out gal-$3^{-/-}$ mice, despite having a parasite burden in the heart that is similar to the burden in wild-type controls, have reduced cardiac cell infiltration and fibrosis. Additionally, in vitro examination of gal-$3^{-/-}$ DCs suggests that the impaired immune response observed in the deficient mice in vivo is a consequence of a deregulated TLR expression in response to the parasite. Taken together, these findings provide a new proinflammatory mechanism for gal-3 in cardiac damage, offering a new rationale for finding new interventional approaches in Chagas cardiomyopathy.

MATERIAL AND METHODS

Animals, Parasites, and Experimental Infection

Trypanosoma cruzi Y strain was used. Epimastigotes were grown in complete liver infusion tryptose medium [25] at 28°C. Intracellular amastigotes were obtained from infected Vero cells. Cell-derived trypomastigotes were collected from the extracellular medium of infected Vero cells, centrifuged (at 2000*g* for 10 minutes), and recovered from the supernatant 3 hours later. Mice aged 6–8 weeks (Harlan Laboratories, Wyton, UK) were infected with 2×10^3 blood trypomastigotes intraperitoneally. gal-$3^{-/-}$ mice, supplied by the Consortium for Functional Glycomics (USA), were maintained and bred under pathogen-free conditions in compliance with European norms [26] in the animal facilities of the Universidad Autonoma (Madrid, Spain). Parasitemia was determined every 2 days by direct counting of parasites in blood.

DC Cultures

DCs were derived by culture of bone marrow cells in complete Roswell Park Memorial Institute 1640 medium supplemented with 10% granulocyte macrophage colony-stimulating factor–transfected X63 myeloma cell line–conditioned medium for 7 days (in 5% CO_2 at 37°C). DCs were either exposed overnight to 1 μg/mL lipopolysaccharide (*Escherichia coli* serotype O26: B6 [Sigma-Aldrich, Dorset, UK]) or cell-derived trypomastigotes (1:10 ratio of DCs to parasites). Cells were collected and washed with cold phosphate-buffered saline (PBS) prior to flow cytometry analysis of surface marker expression. Supernatants were frozen for further cytokine measurement.

Flow Cytometry

Cells were washed, incubated with PBS/10% fetal calf serum and incubated (for 20 minutes at 4°C) with specific antibodies in PBS/0.5% bovine serum albumin (BSA; Sigma-Aldrich) for 30 minutes prior to flow cytometry, with gating according to appropriated isotype controls. The following primary antimouse antibodies were used in accordance with the manufacturer's instructions (BD Pharmingen, Oxford, UK): PE-CD45R/B220, PE-CD4, PE-CD8, PE-Cy5-CD3e, PE-CD11c, FITC-CD11c, FITC-CD80, and FITC-CD86. Alexa-Fluor 488 rabbit antigoat immunoglobulin G (IgG; Molecular Probes, Waltham, Massachusetts) was used in conjunction with antimouse gal-3 (R&D Systems). Purified antibodies against murine TLR1, TLR2, TLR4, and TLR6 (R&D Systems, Boston, Massachusetts) were detected with Alexa Fluor 488 antirat IgG (Molecular Probes). A FACsCalibur flow cytometer (BD Biosciences) was used for data acquisition. Data were analyzed using FlowJo software.

Western Blotting

Heart protein extracts were prepared using a PT 1300 D homogenizer (Polytron) in PBS 0.1% Triton X-100 containing 100 μg/mL pepstatin, 100 μg/mL aprotinin, and 100 μg/mL antipain. Protein concentration was determined by the bicinchoninic acid method (Pierce, Waltham, Massachusetts). Proteins were transferred to nitrocellulose, and membranes were blocked with 5% nonfat milk in Tris-buffered saline plus Tween 20 (TBS-T; 0.5 M NaCl, 20 mM Tris [pH 7.5], and 0.1% Tween-20). Protein loading was visualized by Ponceau staining (Sigma). To detect endogenous gal-3, membranes were incubated with antimouse gal-3 antibody (R&D Systems) in 5% BSA TBS-T (overnight at 4°C) following incubation with horseradish peroxidase–conjugated rabbit antigoat antibody. Specific signals were detected using Supersignal reagent (Pierce). GelAnalyzer2010 software was used for band densitometry.

Quantitative Reverse Transcription–Polymerase Chain Reaction (RT-PCR)

High Pure PCR Template Preparation Kit (Roche, Basel, Switzerland) was used to extract total DNA from cardiac tissue. Total parasite DNA was quantified using quantitative PCR [27]; isolated parasite DNA was used as a calibration curve. RNA was extracted from spleen and heart tissue with Trizol reagent (Invitrogen, Carlsbad, California) and cleaned up (RNeasy Mini Kit, Qiagen, Hilden, Germany). Any residual DNA contamination was removed on column (DNase I, Qiagen). RNA was reverse transcribed into complementary DNA (cDNA; reverse transcriptase; SABiosciences, Frederick, Maryland). The resulting cDNAs were used as template for

subsequent PCR amplification. Gene expression of individual genes was performed using the Real Time SYBR Green PCR Master Mix (SABiosciences). Quantification of gene expression was calculated using the comparative threshold cycle (C_T) method, normalized to GAPDH housekeeping gene (or ribosomal 18S and RPL4 for collagens and laminin) and efficiency of the RT reaction (relative quantity, $2^{-\Delta\Delta CT}$). Analyzed genes and primers are shown in Table 1).

Microscopy and Quantification of Infiltrated Cells in Hearts

Hearts were removed and fixed in 4% paraformaldehyde in PBS before incubation for 24 hours in 30% sucrose. Tissue was then embedded in Tissue-Tek O.C.T. compound (Sakura, Alphen aa den Rijn, the Netherlands). Sections (10 μm) were fixed in paraformaldehyde. Primary antibodies (goat antimouse gal-3 [R&D Systems], rat antimouse CD68 [Serotec, Kidlington, UK], rat antimouse CD4 [eBioscience], and rat anti-mouse CD8 [ebioscience]) were incubated (overnight at 4°C) in PBS/0.5% Triton X-100/1% BSA. Alexa Fluor 488–conjugated rabbit antigoat (Molecular Probes) and Alexa Fluor 555–conjugated goat antirat (Invitrogen) were used for detection. To-Pro3 (Invitrogen) was used for nucleic acid counterstaining. Images were obtained using an Lsm510 Meta Confocal Microscope, and data were analyzed with ImageJ software. Sections were stained with Masson trichrome stain for analysis of collagen distribution and fibrosis.

Cytokine Quantification

FASTQuant microspot assays for cytokine quantification (Whatman, Little Chalfont, UK) was used to detect interleukin 1β (IL-1β), interleukin 5 (IL-5), interleukin 13 (IL-13), interleukin 2 (IL-2), interleukin 6 (IL-6), tumor necrosis factor α (TNF-α), interleukin 4 (IL-4), IL-10, and IFN-γ levels in serum samples according to the manufacturer's instructions. A microarray scanner (Agilent, Santa Clara, California) was used for image acquisition. Evaluation of cytokine levels in cell cultures was conducted using a mouse Th1/Th2 cytometric bead array kit (Bender MedSystems, Vienna, Austria).

Statistical Analysis

Parametric data were analyzed by unpaired, 1-tailed Student *t* tests or 1-way analysis of variance followed by the Newman–Keuls post hoc test. Mann–Whitney *U* (nonparametric) tests were used for analysis of blood parasitemia levels. *P* values of <.05 were considered significant.

RESULTS

gal-3 Is Upregulated in Spleen and Cardiac Tissue During Infection

Consistent with previous reports [20], we observed a clear upregulation of gal-3 in C57BL/6 mice in response to infection (Figure 1*A*–*F*). gal-3 messenger RNA (mRNA) levels were increased upon infection in splenocytes (Figure 1*A*), and consistent results were observed at the protein level, reaching maximum levels at day 21 after infection (Figure 1*B*). In accordance with previous reports, gal-3 was expressed mostly by antigen-presenting cells in spleens of noninfected mice (data not shown), whereas *T. cruzi*–mediated upregulation of gal-3 was dependent on T and B lymphocytes (Figure 1*C*). gal-3 was also detected in the heart of infected mice, both at the mRNA level (Figure 1*D*)

Table 1. List of Primers Used in the Study

Gene	Reference Sequence	Forward Primer	Reverse Primer
Galectin-1	NM_008495.2	CTCAAAGTTCGGGGAGAGGT	CATTGAAGCGAGGATTGAAGT
Galectin-2	NM_025622.1	CTAGGAGCAACTGGGAGAGC	CCCTGGTTTCATGTTCAGGT
Galectin-3	NM_010705.1	GCCTACCCCAGTGCTCCT	GGTCATAGGGCACCGTCA
Galectin-4	NM_010706.1	CATGCCTGAGCACTACAAGG	CGAGGAAGTTGATGGACTGAA
Galectin-8	NM_018886.2	GCATGTCCCTAAAGATTCAGAAA	GACCTTTTGAACCGAGGGTTA
Galectin-9	NM_010708.1	ACCCTACCACCTCGTGGAC	ACCCTACCACCTCGTGGAC
TLR2	NM_011905	GGGGCTTCACTTCTCTGCTT	AGCATCCTCTGAGATTTGACG
TLR4	NM_021297	GGACTCTGATCATGGCACTG	CTGATCCATGCATTGGTAGGT
IL-5	NM_010558	ACATTGACCGCCAAAAAGAG	ATCCAGGAACTGCCTCGTC
NOS	NM_010927	CTTTGCCACGGACGAGAC	TCATTGTACTCTGAGGGCTGAC
Arg1	NM_007482	GAATCTGCATGGGCAACC	GAATCCTGGTACATCTGGGAAC
GAPDH	NM_008084	ACCCAGAAGACTGTGGATGG	ACACATTGGGGGTAGGAACA
COX-2	NM_011198	GATGCGCTTCCGAGCTGTG	GGATTGGAACAGCAAGGATTT
mCOL1	NM_007743	GAAACCCGAGGTATGCTTGA	GAGACCACGAGGACCAGAAG
mCOLIV	NM_009930	CAAGCATAGTGGTCCGAGTC	AGGCAGGTCAAGTTCTAGCG
mCOLIII	NM_007736	GTTCTAGAGGATGGCTGTACTAAACACA	TTGCCTTGCGTGTTTGATATTC
mRPL4	NM_024212.4	AGCAGCCGGGTAGAGAGG	ATGACTCTCCCTTTTCGAGT
m18SRNA	NR_003278.3	CGGACAGGATTGACAGATTG	CAAATCGCTCCACCAACTAA
mLama1	NM_008480	TGTAGATGGCAAGGTCTTATTTCA	CTCAGGCAGTTCTGTTTGATGT

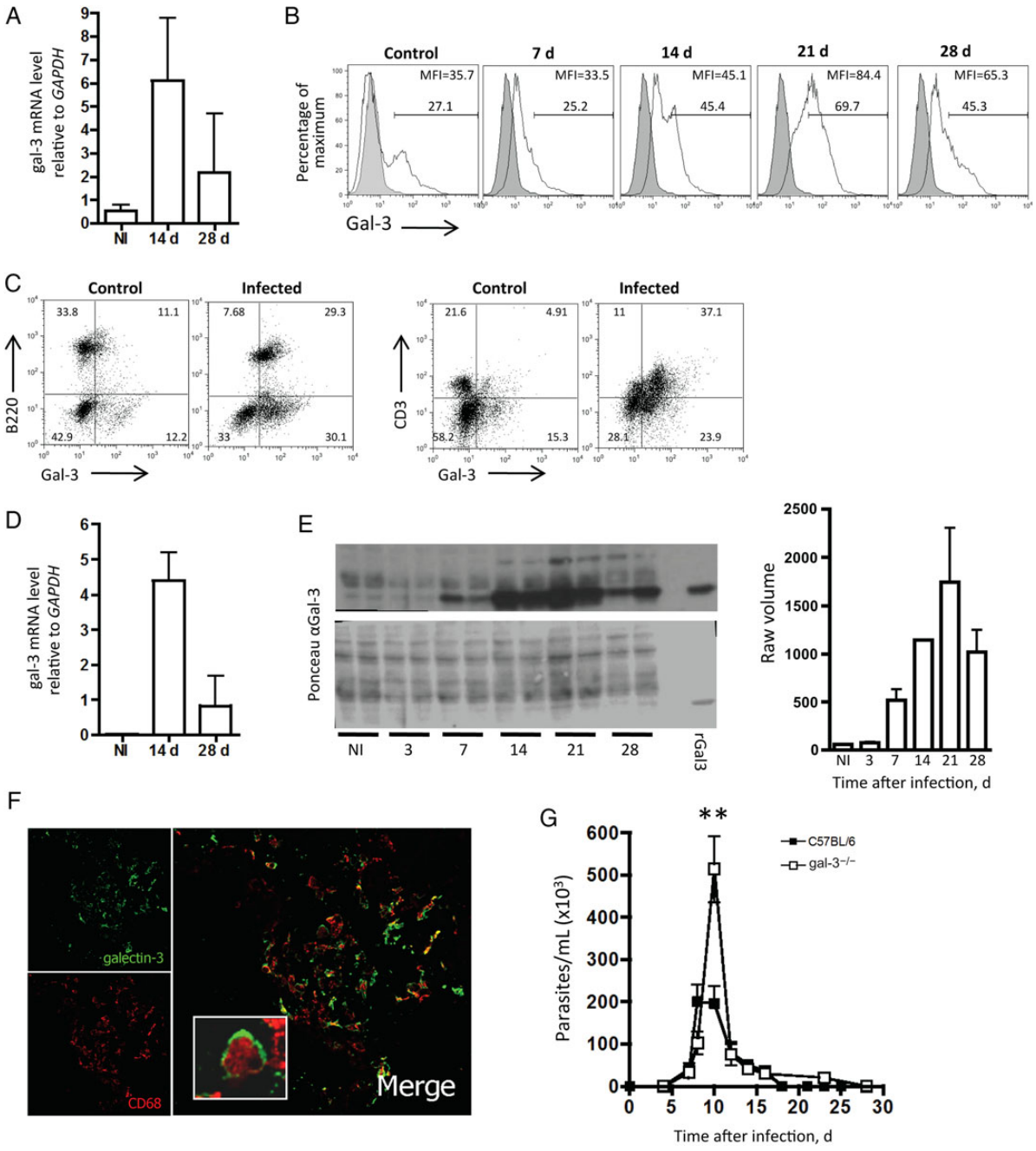

Figure 1. *Trypanosoma cruzi* induces galectin-3 (gal-3) expression in spleen cells and cardiac tissue and controls the number of circulating parasites. C57BL/6 mice were infected with *T. cruzi* blood trypomastigotes Y strain (day 0). *A*, Spleen cells from individual mice (n = 5) were isolated and pooled to quantify relative expression of gal-3 messenger RNA (mRNA) by reverse transcription–polymerase chain reaction (RT-PCR). *B*, Infected mice were culled weekly to analyze surface gal-3 expression on spleen cells by fluorescence-activated cell-sorting analysis (open histograms), compared with isotype controls (tinted histograms). Numbers represent percentages of positive cells in pooled samples (n = 5) and mean fluorescence intensities (MFIs). *C*, Spleen cells from individual mice (n = 5) were pooled to evaluate gal-3 expression (*x*-axis) in $B220^+$ or $CD3^+$ cells (*y*-axis) in noninfected and infected mice (21 days after infection). *D*, mRNA was extracted from cardiac tissue (5 pooled mice) and levels of gal-3 mRNA relative expression were evaluated by RT-PCR. *E*, Cardiac tissue from noninfected control mice (NI) and infected mice (7, 14, 21, and 28 days after infection) were analyzed by Western blotting (upper panel) to quantify gal-3 expression. A Ponceau-stained specimen (lower panel) is shown as a loading control, and purified recombinant gal-3 (rGal3) was used as positive control to confirm antibody selectivity. Each lane shows 5 pooled hearts from 2 independent experiments. Densitometry of bands corresponding to gal-3 expression is shown on the right. Results show normalized gal-3 expression to total protein Ponceau staining. Error bars represent mean ± SD. *F*, Heart sections from a representative infected mouse (14 days after infection) were stained for $CD68^+$ (red) and gal-3 (green). Isotype control sections were negative for both markers. *G*, Blood parasitemia level was quantified by direct counting under optical microscopy every 2 days. Data represent the mean values ± standard errors of the mean for individual mice (n = 15) from 3 independent experiments. Error bars in panels *A* and *D* represent the mean of 2 independent experiments, using pooled samples from individual mice (n = 5). $^{**}P < .01$.

and the protein level (Figure 1*E*), showing a peak of expression at day 21 after infection, in contrast to the absence of gal-3 expression in noninfected mice. By colocalization studies, gal-3 was found to be expressed by infiltrating $CD68^+$ macrophages (Figure 1*F*). Overall, these data suggest that gal-3 might play a relevant role in immunity against *T. cruzi*, not only at systemic levels, but also at local site of inflammation, such as cardiac tissue.

To further investigate the role of gal-3 in modulating responses against *T. cruzi*, C57BL/6 and gal-3 knockout (gal-$3^{-/-}$) mice were infected. Interestingly, whereas gal-$3^{-/-}$ mice presented a significant (2.5-fold) increase in the number of parasites at day 10 after infection, they were still able to eliminate circulating parasites at later stages similarly to wild-type controls (Figure 1*G*). This perhaps suggests that gal-3 is not involved in acquired immunity, which becomes fully activated approximately 10–15 days following infection, but in earlier immune events coinciding with activation of innate immune responses.

gal-3 Modulates Systemic Immune Responses Against *T. cruzi*

gal-3 has been described as a pattern-recognition receptor [17], and in line with this, we have recently shown that gal-3 binds specifically to infective forms of *T. cruzi* [28]. Therefore, we hypothesized that the increased number of parasites in blood observed in gal-$3^{-/-}$ mice could be a reflection of inefficient early parasite recognition. Moreover, we observed that splenocytes from infected mice showed a significantly increased ability to bind recombinant gal-3 (data not shown), indicating that *T. cruzi* induces expression of gal-3 endogenous ligands in immune cells, perhaps as a resulting change in the glycosylation pattern during infection that, along with the increased expression of gal-3, might sensitize immune cells to gal-3–mediated actions. Corroborating this hypothesis, levels of proinflammatory cytokines in serum specimens from gal-$3^{-/-}$ infected mice were dramatically reduced (Figure 2*A*). Expression of signature cytokines for both Th1 and Th2 responses, IFN-γ and IL-5, respectively, were equally inhibited. Similarly, reduced levels of IL-6 and IL-10 were observed; TNF-α was only reduced at day 28 after infection, suggesting that gal-3–mediated modulation of systemic responses might be specific to certain cell types and/or disease stages.

To further address the mechanisms underlying such immunosuppression, we analyzed gene expression in spleens (Figure 2*B*). Infection induced mRNA expression of other galectins in wild-type mice and, albeit to a lesser extent, in gal-$3^{-/-}$ mice. In accordance with cytokine mRNA levels in serum specimens, IL-5 and IFN-γ were also significantly reduced at the mRNA level in splenocytes from infected gal-$3^{-/-}$ mice. Interestingly, TLR4 expression was significantly downregulated in gal-$3^{-/-}$ mice. Genes involved in the response against *T. cruzi,* like inducible nitric oxide synthase (iNOS), arginase I, or COX-2 were also downregulated, although no statistical significance was reached (data not shown). The observed low IFN-γ expression in gal-$3^{-/-}$ mice might still be able to activate macrophages to induce iNOS as a result of similarly reduced levels of the inhibitory cytokines IL-10 and IL-5, perhaps explaining why gal-$3^{-/-}$ mice are able to control parasitemia during the late resolution phase (Figure 1*G*). Of note, differential gene expression in spleens from gal-$3^{-/-}$ infected mice was not likely to be a result of expansion of any particular cell type, since no major differences were observed with respect to wild-type mice regarding total cell counts (Figure 2*C*) or proportions of cell populations in spleens (Figure 2*D*).

Infected gal-$3^{-/-}$ Mice Show Reduced Cell Infiltration and Fibrosis in the Heart Despite Having a Similar Parasite Burden

Our results show that gal-3 regulates systemic responses during infection. However, cardiac tissue, the main target in Chagas disease, presents differential inflammatory networks that can potentially affect gal-3–mediated actions. Therefore, it was essential to understand the contribution of gal-3 to local cardiac inflammation, specially considering the increasing evidence of gal-3 as a biomarker in cardiac pathology. Hence, we next decided to investigate the potential role of gal-3 in the heart of infected animals by evaluating mRNA gene expression (Figure 3*A*). Interestingly, expression of other galectins was upregulated during infection in wild-type animals, suggesting that other members of the galectin family may play a relevant role in Chagas immunopathology. Contrary to the results observed in splenocytes, galectin expression was induced in heart of gal-$3^{-/-}$ animals, compared with wild-type cohorts, perhaps suggestive of some compensatory mechanism in the knockout animals. However, gal-3 is the only chimera-type galectin, and it is unlikely that other galectins can mimic gal-3–mediated actions. Expression of TLR2 and TLR4 were highly induced in gal-$3^{-/-}$ mice, and no differences were observed in IFN-γ and IL-5 expression (Figure 3*A*), in contrast to the results observed in spleens, indicating that gal-3–dependent effects strongly depend on particular microenvironments. Furthermore, whereas expression of iNOS mRNA was significantly downregulated in hearts from gal-$3^{-/-}$ mice, expression of other immune genes, such as arginase or COX-2, remained unaffected (Figure 3*A* and data not shown). On the basis of these results, we concluded that gal-3 was involved in controlling cardiac inflammation.

We next decided to evaluate the number of infiltrating cells in the heart of infected animals. Strikingly, gal-$3^{-/-}$ mice showed a reduced number of infiltrating $CD68^+$ macrophages, $CD4^+$ and $CD8^+$ T cells (Figure 3*B*). The observed defect in cell migration did not appear to be related to any major chemokine-related pathways, as we were not able to find any difference in expression of CXCR12, Ccr2, Ccr5, ICAM1, integrin α, or selectins (data not shown). To assess the contribution of gal-3 to parasite proliferation, we quantified the amount of *T. cruzi* DNA in cardiac tissue. Despite the attenuated immune response observed in gal-$3^{-/-}$ mice, they still presented a parasite burden similar

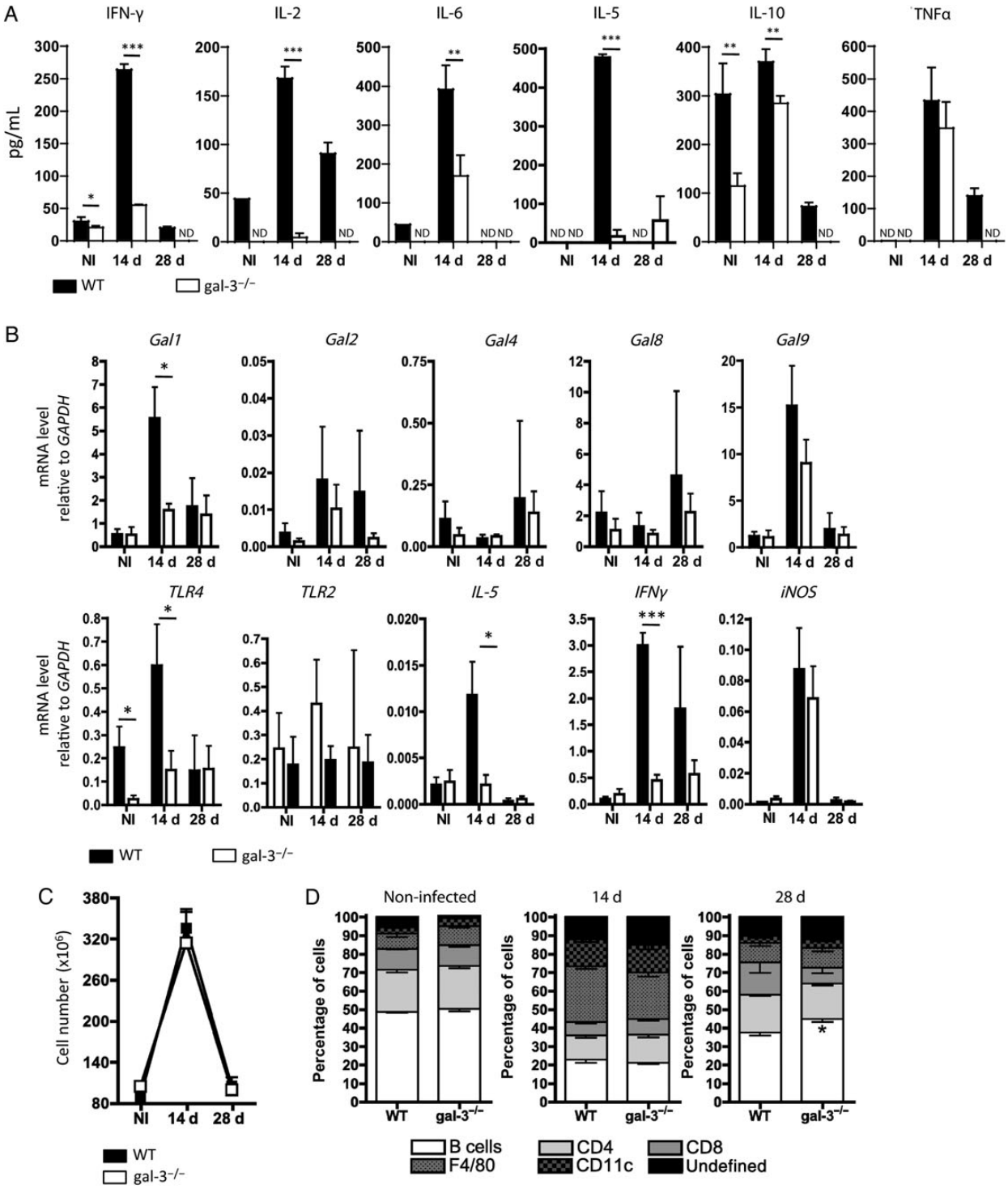

Figure 2. Galectin-3–deficient (gal-3$^{-/-}$) mice have downregulated systemic immune response. Wild-type (WT) C57BL/6 and gal-3$^{-/-}$ mice were infected with *Trypanosoma cruzi* trypomastigotes. *A*, Cytokine levels in serum were analyzed as described in "Material and Methods" section in noninfected mice (NI) and infected mice (14 and 28 days after infection). *B*, *gal-1, gal-2, gal-3, gal-4, gal-8, gal-9, TLR4, TLR2, IL-5, IFNγ*, and *iNOS* messenger RNA levels were evaluated in control noninfected mice (NI) and infected mice (14 and 28 days after infection). Results are expressed as relative levels to *GADPH*. For a list of primers used see Table 1. For panels *A* and *B*, values show the mean ± standard deviation (SD) of 3 independent experiments, in which samples were pooled from individual mice (n = 5) and analyzed in triplicate. *C*, Total number of cells in spleens from control noninfected mice and infected mice (14 and 28 days after infection). *D*, Percentages of B220^{+}, CD4^{+}, CD8^{+}, F4/80^{+}, and CD11c^{+} spleen cells were quantified by flow cytometry, using relevant isotype controls for the gating strategy. For panels *C* and *D*, data are the mean values ± SD for 10 individual mice from 3 independent experiments. Unless specified, black columns and symbols represent C57BL/6 mice, and white columns and symbols represents gal-3$^{-/-}$ mice. **P* < .05, ***P* < .01, and ****P* < .001. Abbreviation: ND, not detected.

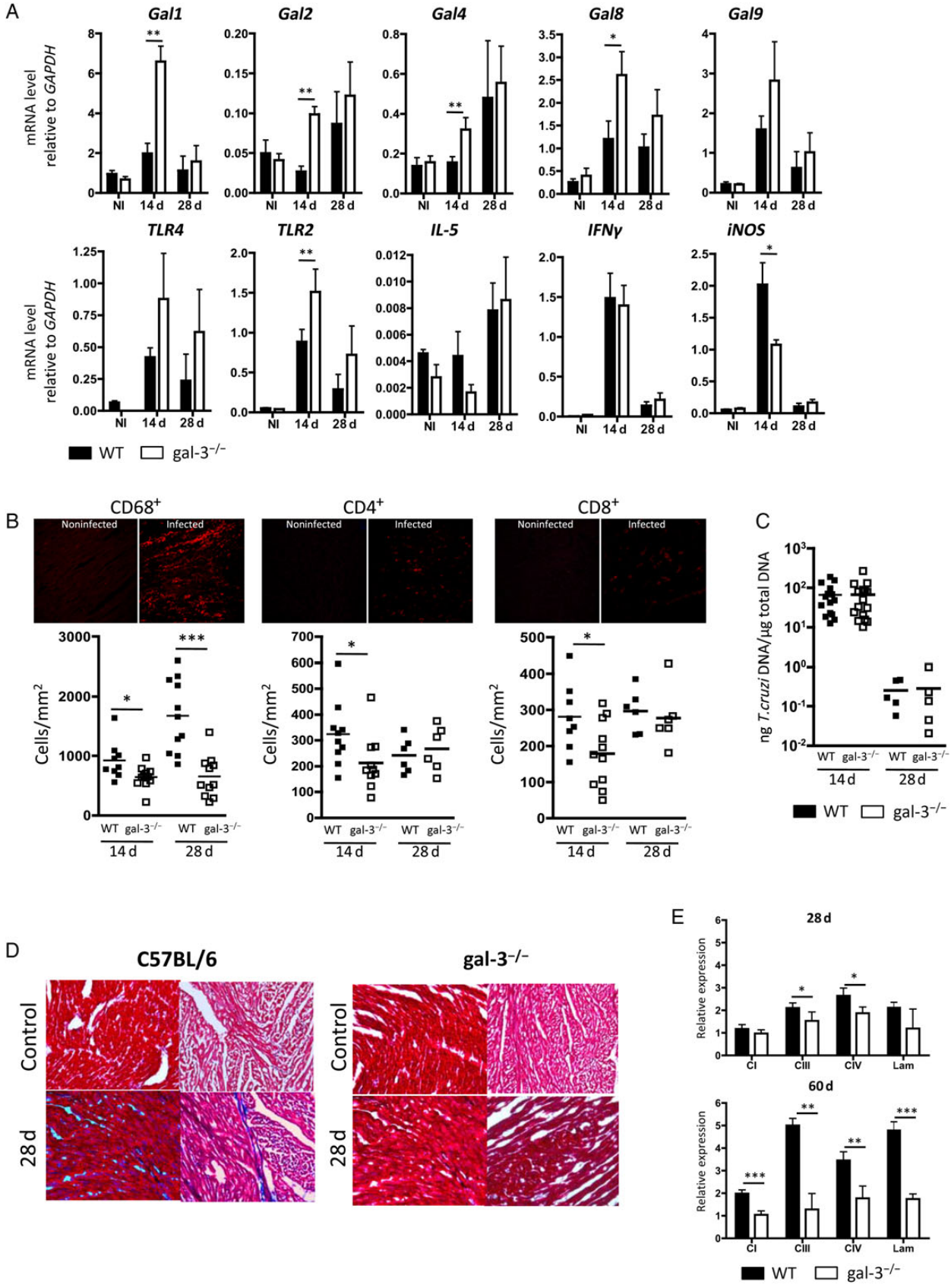

Figure 3. Galectin-3–deficient (gal-3$^{-/-}$) mice present diminished cell infiltration and collagen deposition in the heart in response to similar parasite burdens. *A*, Heart gene expression during infection. *gal-1, gal-2, gal-3, gal-4, gal-8, gal-9, TLR4, TLR2, IL-5, IFNγ*, and *iNOS* messenger RNA levels, relative

to that in the control C57BL/6 mice (Figure 3*C*), in clear contrast to the increased parasitemia levels observed in blood specimens but consistent with the ability of gal-3$^{-/-}$ mice to eliminate circulating parasites at later stages (Figure 1*G*).

Since cardiac damage has been attributed to parasite persistence and self-damaged inflammatory responses, it was important to evaluate pathophysiological changes such as tissue remodeling and fibrosis. As expected, infection in wild type mice caused fibrosis and accumulation of collagen in the cardiac interstitium representative of tissue damage, but gal-3$^{-/-}$ animals presented significant reduced levels (Figure 3*D*). This result was corroborated by reduced expression of collagens I, III, IV, and laminin in the heart of gal-3$^{-/-}$ infected animals (Figure 3*E*), suggesting that cardiac fibrosis in Chagas disease might be a result of the upregulated expression of gal-3 in cardiac tissue, rather than of parasite persistence.

gal-3 Is Necessary to Induce Proinflammatory Responses in DCs in Response to *T. cruzi*

gal-3-dependent effects appeared to be tissue specific, as reflected by the distinctive regulation of TLR and galectin expression in heart and spleen. To investigate the mechanism underlying the in vivo observations, we studied the role of gal-3 in DCs, as they are essential to initiating immune responses against *T. cruzi* [29]. We hypothesized that the phenotype observed in infected gal-3$^{-/-}$ mice could be a consequence of inadequate DC immunoregulatory abilities, such as cell activation or costimulatory properties, that are associated with TLR activation. DCs upregulated gal-3 expression after incubation with trypomastigotes (Figure 4*A*), as previously reported [20]. To evaluate the role of gal-3 in DC activation, cells were exposed to cell-derived trypomastigotes or LPS, and expression of costimulatory molecules was assessed. Interestingly, gal-3$^{-/-}$ DC failed to induce CD80 expression in response to the parasite (Figure 4*B*), whereas CD86 was not affected (data not shown). Furthermore, gal-3$^{-/-}$ DCs showed reduced IL-1 and TNF-α production upon exposure to trypomastigotes (Figure 4*C*), corroborating the immunosuppressed phenotype observed in vivo.

The Decreased Proinflammatory Response of gal-3$^{-/-}$ DCs Is Associated With Impaired TLR Expression

As it is well known that DCs are activated by *T. cruzi* through TLR activation to produce IL-1 and TNF-α [9, 30–32], we hypothesized that the reduced cytokine production of gal-3$^{-/-}$ DCs was a result of a deregulated expression of TLRs. To assess this, expression of TLR1, TLR2, TLR4, and TLR6 on wild-type and gal-3$^{-/-}$ DCs was measured in the presence and absence of *T. cruzi* trypomastigotes. No differences were found among groups without parasites, and all of the TLRs tested were upregulated in the wild-type DCs after incubation with *T. cruzi* (Figure 5). By contrast, whereas TLR1 and TLR4 were poorly induced on the surface of gal-3$^{-/-}$ DCs in response to *T. cruzi*, TLR2 and TLR6 maintained similar expression levels as the wild-type DCs. These results were confirmed at mRNA level (data not shown), suggesting that gal-3 controls DCs responses to trypomastigotes via TLR1/2 and TLR4-dependent mechanisms. Surprisingly, when DCs were incubated with purified intracellular amastigotes, no significant differences in TLR expression were observed in cells from gal-3$^{-/-}$ mice (data not shown), reflecting the distinctive nature of the glycoconjugates found in *T. cruzi* biological forms and suggesting again that gal-3 is involved mostly in early innate immunity against *T. cruzi,* in line with the proposed TLR2-dependent immunity during early infection stages [33].

DISCUSSION

Collectively, our findings suggest a role for gal-3 in cardiac fibrosis during Chagas disease that is in line with the increasing interest in this protein as potential target of drug development in cardiomyopathy [34, 35]. In fact, gal-3 is a strong proinflammatory mediator [36], and it is induced in B cells, DCs, and macrophages upon *T. cruzi* infection [19, 20, 37]. Of note, galectins might require special consideration in Chagas disease, as the enzyme trans-sialidase, expressed by *T. cruzi*, is able to transfer sialic acid from host cells to parasite glycans, modulating sialylation of terminal galactose residues and, thus, consequent galectin-derived effects, in a similar way that different

Figure 3 continued. to GAPDH, in infected mice (14 and 28 days after infection) and control noninfected mice. Data represent mean values ± SD of samples pooled from individual mice (n = 5) from 3 independent experiments. *B*, Quantification of immune cells infiltrating cardiac tissue. Images represent heart tissue sections from 1 representative wild-type (WT) mouse from the noninfected and infected groups (14 days after infection), stained with anti-CD4, anti-CD8, or anti-CD68 antibodies. Graphs show quantification of CD4$^+$, CD8$^+$, or CD68$^+$ cells of individual hearts, where each dot represents individual samples, shown as the mean of 5 independent fields counted separately. *C*, Quantification of *Trypanosoma cruzi* DNA in heart tissue specimens from infected mice. Total DNA was isolated from heart on the indicated days after infection, and quantitative polymerase chain reaction for *T. cruzi* DNA was performed. Symbols represent data from individual mice. *D*, Diminished collagen deposition in hearts from gal-3$^{-/-}$ mice, compared with WT controls. Representative photomicrographs of Masson trichrome–stained sections from control and *T. cruzi*–infected (28 days after infection) C57BL/6 (left panel) and gal-3$^{-/-}$ (right panel) mice for pathological evaluation. Collagen fibers are stained in blue. *E*, Expression of collagens I, III, and IV and laminin in mouse heart tissue specimens during *T. cruzi* infection. Total RNA was isolated in heart tissue specimens obtained from infected (28 and 60 days after infection) C57BL/6 and gal-3$^{-/-}$ mice. Data were analysed as relative levels to ribosomal 18S and RPL4 and normalized to noninfected relavant controls. Experiment was done in duplicate using pooled DNA from 4 individual mice. Black columns and symbols represent C57BL/6 mice, and white columns and symbols represent gal-3$^{-/-}$ mice. $^*P < .05$, and $^{**}P < .01$, $^{***}P < .001$.

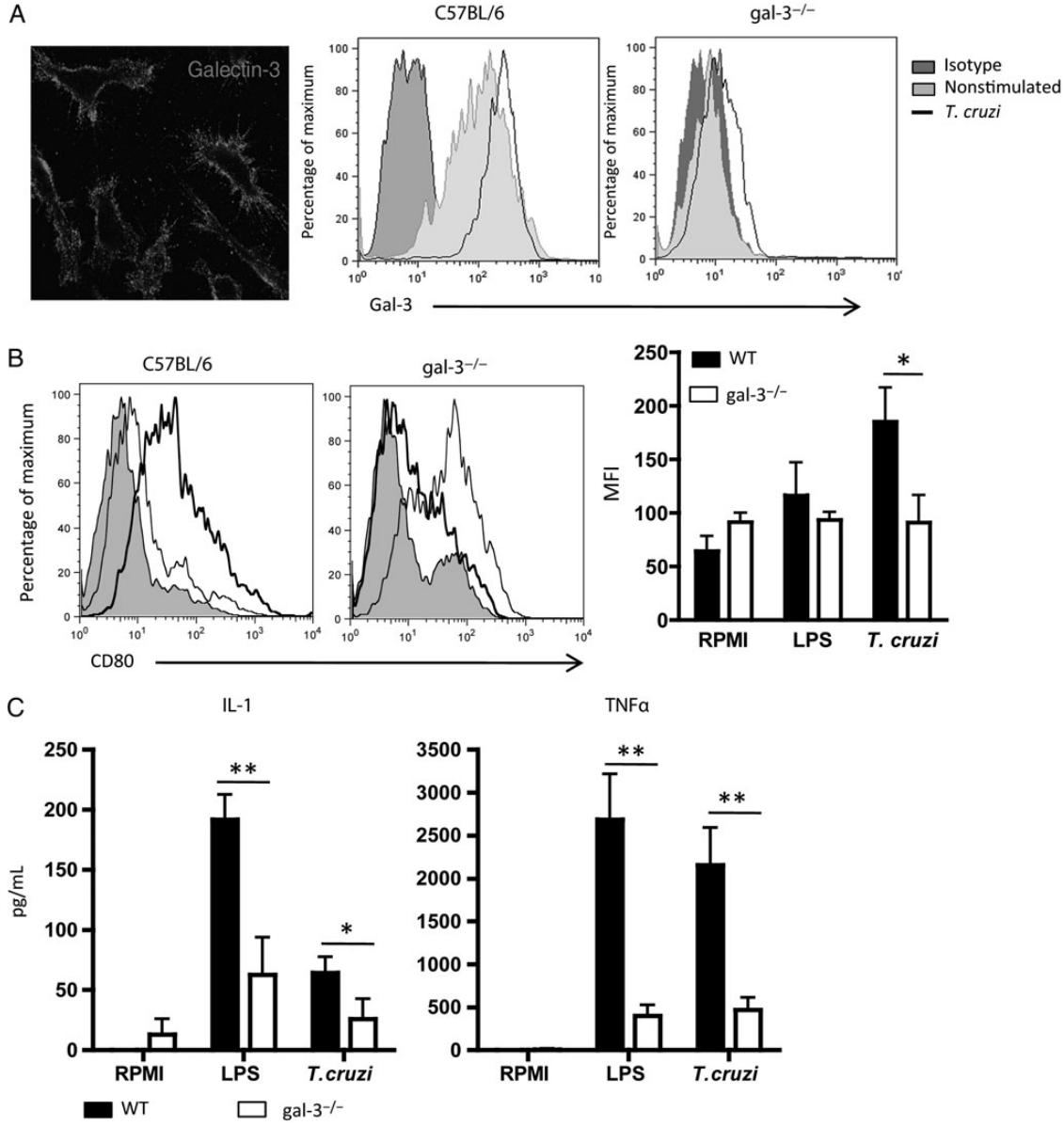

Figure 4. Dendritic cells (DCs) from galectin-3–deficient (gal-$3^{-/-}$) mice show reduced cytokine synthesis in response to *Trypanosoma cruzi*, along with reduced CD80 expression in vitro. *A*, DCs upregulate gal-3 in response to *T. cruzi*. gal-3 was detected on DCs from C57BL/6 mice by immunofluorescence analysis (left panel) and by flow cytometry under basal and lipopolysaccharide (LPS)–stimulated conditions (middle panel). gal-$3^{-/-}$ DCs were not stained under the same conditions (right panel). Histograms show gal-3 expression in noninfected cells (light gray) and cells exposed to *T. cruzi* trypomastigotes (black line). Negative isotype controls are shown (dark gray). *B*, DCs were analyzed for surface expression of CD80 by flow cytometry. Histograms show nontreated (gray), LPS-stimulated (thin black line), and *T. cruzi*–stimulated (thick black line) cells from 1 representative experiment. Panels in the right represent mean fluorescent intensities (MFIs) ± SD from 3 independent experiments. *C*, Cytokine production by DCs in response to LPS and *T. cruzi* trypomastigotes. Interleukin 1 (IL-1) and tumor necrosis factor α (TNF-α) levels were evaluated in the supernatant of cell cultures of wild-type mouse DCs (black columns) and gal-$3^{-/-}$ mouse DCs (white columns). Data show mean values ± SD of 3 independent experiments analyzed in triplicate. For panels *B* and *C*, DCs were incubated overnight with LPS (1 μg/mL) or *T. cruzi* trypomastigotes (parasite to cell ratio, 10:1). **P* < .05, ***P* < .01, and ****P* < .001. Abbreviation: RPMI, Roswell Park Memorial Institute 1640 medium.

sialylation levels regulate gal-1–mediated apoptosis of Th1/Th17 but not Th2 cells [38]. However, little is still known about how gal-3 affects initiation and/or resolution of the immune response against the parasite.

We show here that gal-$3^{-/-}$ mice have reduced levels of proinflammatory cytokines upon infection. This suggests that gal-3 is essential to initiate systemic innate immune responses, since both Th1 and Th2 responses were equally affected,

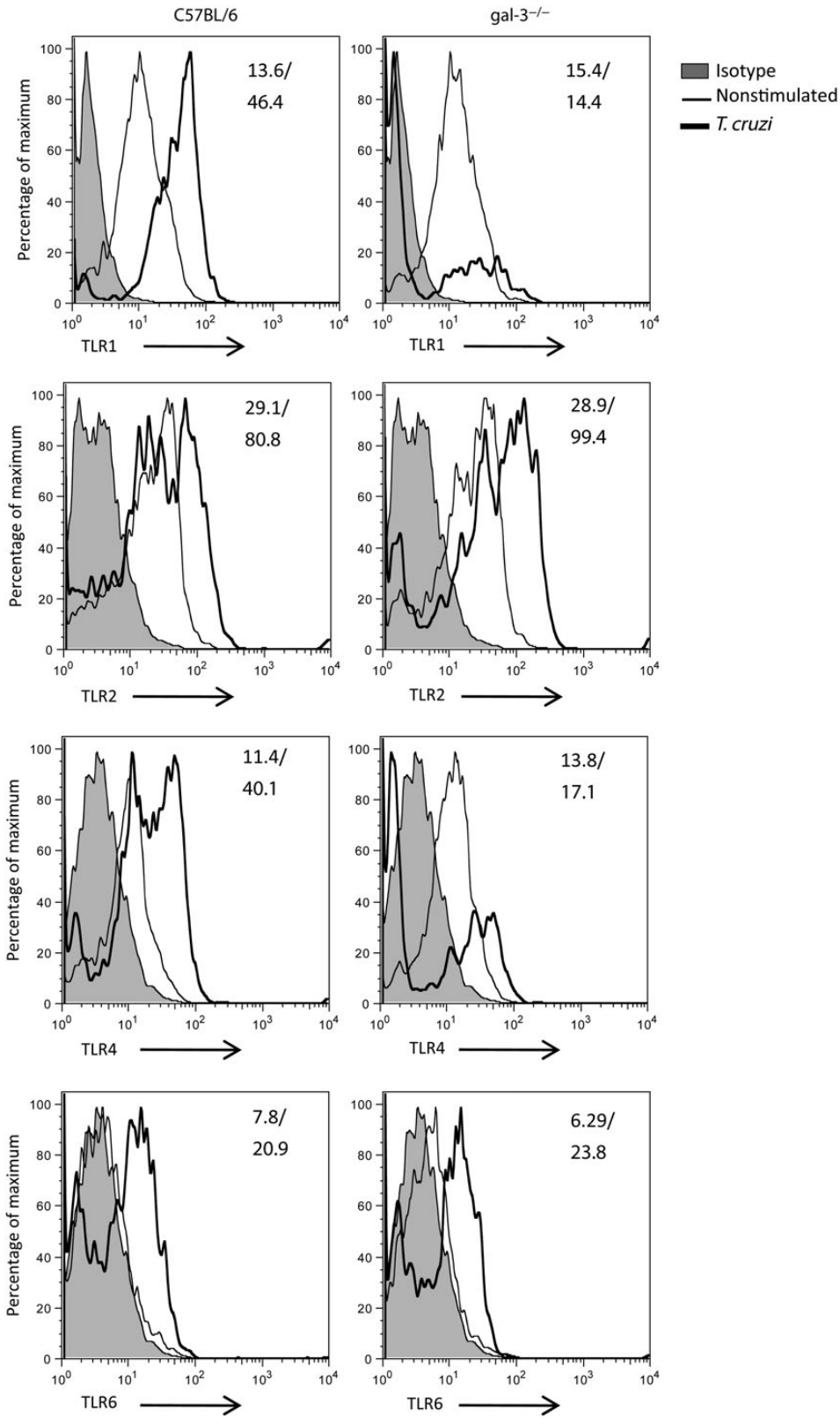

Figure 5. Toll-like receptor (TLR) surface expression is impaired on dendritic cells (DCs) from galectin-3–deficient (gal-$3^{-/-}$) mice after *Trypanosoma cruzi* infection. Expression of Toll-like receptor 1 (TLR1), TLR2, TLR4, and TLR6 was determined by flow cytometry. Expression levels relative to isotype control (gray histograms) are shown for nontreated cells in the absence of the parasite (thin line) or for cells cultured overnight in the presence of *T. cruzi* trypomastigotes (thick line; ratio of DCs to parasites, 1:10). Figure shows a representative result of 2 independent experiments. Numbers represent mean fluorescence intensities of nontreated cells versus cells incubated with *T. cruzi* (bold text).

perhaps because of the role of gal-3 in synapse formation between antigen-presenting cells and naive T cells [39] and production of IL-2 by activated lymphocytes [40]. However, the observed reduction in cytokine expression did not seem to be a consequence of differential relative expansion or reduction of any immune cell population, since the lack of gal-3 did not affect significantly the relative proportion of the major immune cell compartments in spleens.

Surprisingly, although gal-$3^{-/-}$ mice did not present any change in the number of parasites in the heart, they had a dramatically reduced number of infiltrating macrophages, $CD4^+$ T lymphocytes, and $CD8^+$ T lymphocytes. Supporting this, exogenous gal-3 significantly increased macrophage migration in some in vitro models [41]. Hence, gal-3 may trigger self-destructive mechanisms to initiate cardiac inflammation and perhaps subsequent CCC. Of note, expression of gal-3 in fibroblasts and macrophages in animal models has been linked to fibrosis and cardiac remodeling in failure-prone hypertrophied hearts [42], pathology that strongly resembles CCC. Indeed, we have shown here that gal-$3^{-/-}$ mice have diminished cardiac fibrosis, despite having a similar parasite burden in the heart. Similarly, gal-3 expression is sufficient to mediate the development of heart failure [43], and pharmacological inhibition of gal-3 attenuates cardiac fibrosis [44].

Collectively, therefore, our data provide compelling evidence for a proinflammatory role for gal-3 in Chagas disease, indicative of its ability to promote tissue inflammation, cell infiltration, and cardiac damage. Gene expression showed upregulated expression of TLRs in hearts from gal-$3^{-/-}$ mice, and interestingly, TLR2 is the main upstream regulator of IL-1–mediated hypertrophy triggered by *T. cruzi* in isolated cardiomyocytes [45]. However, TLR expression in spleen followed an opposite trend, perhaps reflecting the differences observed in systemic and local responses due to specific inflammatory microenvironments.

Our data suggest that the immune alterations observed in gal-$3^{-/-}$ infected animals can be, at least in part, due to a defective response of DCs in virtue of the deregulated expression of TLR1 and TLR4 observed in gal-$3^{-/-}$ DCs, resulting in diminished cell activation. This finding represents a new mechanism of gal-3 to regulate TLR-dependent responses, perhaps by binding and cross-linking glycans expressed in TLRs to modulate effector responses, as activation of MyD88-associated pathways is dependent on the dimerization of TLR4 molecules, a process occurring after removal of α-2,3-sialyl residue from glycans expressed in TLR4 [46]. Also, the decreased TLR1 expression in gal-$3^{-/-}$ DCs may affect TLR2 signaling by disrupting the functional heterodimer TLR1/2 [47] required for the immune response against *T. cruzi* [9, 32, 48, 49], particularly during early disease stages [33], correlating with the observed impaired cytokine production in gal-$3^{-/-}$ DCs and the diminished leukocyte recruitment in the heart of gal-$3^{-/-}$ animals that are attributed to the activation of TLR2 by mucins from the protozoan [21]. Interestingly, cooperative signaling via TLR4 and TLR2 induced the synergy in DCs production of antiinflammatory IL-10 [50], process that may be mediated by gal-3.

Although full understanding of the mechanisms underpinning gal-3–driven systemic and local inflammation requires further exploration, we provide evidence here that gal-3 is regulating specific TLR expression during *T. cruzi* infection to orchestrate inflammatory responses against the parasite but that it also mediates macrophage and lymphocyte infiltration in chagasic hearts to induce fibrosis and subsequent cardiac damage, suggesting that gal-3 is a potential target to treat pathogenic inflammatory reactions in CCC.

Notes

Financial support. This work was supported by the Instituto de Salud Carlos III within the Network of Tropical Diseases Research (VI P I+D+I 2008-2011, ISCIII-Subdirección General de Redes y Centros de Investigación Cooperativa [RD12/0018/0009]); the Fondo de Investigaciones Sanitarias (grants PI11/00033 and PI14/00184); and Fundación Ramón Areces (CBMSO institutional grant).

Potential conflicts of interest. All authors: No reported conflicts.

All authors have submitted the ICMJE Form for Disclosure of Potential Conflicts of Interest. Conflicts that the editors consider relevant to the content of the manuscript have been disclosed.

References

1. Mathers CD, Ezzati M, Lopez AD. Measuring the burden of neglected tropical diseases: the global burden of disease framework. PLoS Negl Trop Dis **2007**; 1:e114.
2. Tarleton RL. Parasite persistence in the aetiology of Chagas disease. Int J Parasitol **2001**; 31:550–4.
3. Zhang L, Tarleton RL. Parasite persistence correlates with disease severity and localization in chronic Chagas' disease. J Infect Dis **1999**; 180:480–6.
4. Girones N, Cuervo H, Fresno M. *Trypanosoma cruzi*-induced molecular mimicry and Chagas' disease. Curr Top Microbiol Immunol **2005**; 296:89–123.
5. Levin MJ, Kaplan D, Ferrari I, Arteman P, Vazquez M, Panebra A. Humoral autoimmune response in Chagas' disease: *Trypanosoma cruzi* ribosomal antigens as immunizing agents. FEMS Immunol Med Microbiol **1993**; 7:205–10.
6. Soares MB, Pontes-De-Carvalho L, Ribeiro-Dos-Santos R. The pathogenesis of Chagas' disease: when autoimmune and parasite-specific immune responses meet. An Acad Bras Cienc **2001**; 73:547–59.
7. Girones N, Fresno M. Etiology of Chagas disease myocarditis: autoimmunity, parasite persistence, or both? Trends Parasitol **2003**; 19:19–22.
8. Kierszenbaum F. Where do we stand on the autoimmunity hypothesis of Chagas disease? Trends Parasitol **2005**; 21:513–6.
9. Bafica A, Santiago HC, Goldszmid R, Ropert C, Gazzinelli RT, Sher A. Cutting edge: TLR9 and TLR2 signaling together account for MyD88-dependent control of parasitemia in *Trypanosoma cruzi* infection. J Immunol **2006**; 177:3515–9.
10. Tarleton RL. Immune system recognition of *Trypanosoma cruzi*. Curr Opin Immunol **2007**; 19:430–4.
11. Cuervo H, Pineda MA, Aoki MP, Gea S, Fresno M, Girones N. Inducible nitric oxide synthase and arginase expression in heart tissue during acute *Trypanosoma cruzi* infection in mice: arginase I is expressed in infiltrating CD68+ macrophages. J Infect Dis **2008**; 197:1772–82.
12. Rocha Rodrigues DB, dos Reis MA, Romano A, et al. In situ expression of regulatory cytokines by heart inflammatory cells in Chagas' disease patients with heart failure. Clin Dev Immunol **2012**; doi:10.1155/2012/361730.

13. de Oliveira GM, Diniz RL, Batista W, et al. Fas ligand-dependent inflammatory regulation in acute myocarditis induced by *Trypanosoma cruzi* infection. Am J Pathol **2007**; 171:79–86.
14. Almeida IC, Camargo MM, Procopio DO, et al. Highly purified glycosylphosphatidylinositols from *Trypanosoma cruzi* are potent proinflammatory agents. EMBO J **2000**; 19:1476–85.
15. Cardillo F, Voltarelli JC, Reed SG, Silva JS. Regulation of *Trypanosoma cruzi* infection in mice by gamma interferon and interleukin 10: role of NK cells. Infect Immun **1996**; 64:128–34.
16. Liu FT, Yang RY, Hsu DK. Galectins in acute and chronic inflammation. Ann N Y Acad Sci **2012**; 1253:80–91.
17. Kohatsu L, Hsu DK, Jegalian AG, Liu FT, Baum LG. Galectin-3 induces death of Candida species expressing specific beta-1,2-linked mannans. J Immunol **2006**; 177:4718–26.
18. Quattroni P, Li Y, Lucchesi D, et al. Galectin-3 binds Neisseria meningitidis and increases interaction with phagocytic cells. Cell Microbiol **2012**; 14:1657–75.
19. Acosta-Rodriguez EV, Montes CL, Motran CC, et al. Galectin-3 mediates IL-4-induced survival and differentiation of B cells: functional cross-talk and implications during *Trypanosoma cruzi* infection. J Immunol **2004**; 172:493–502.
20. Vray B, Camby I, Vercruysse V, et al. Up-regulation of galectin-3 and its ligands by *Trypanosoma cruzi* infection with modulation of adhesion and migration of murine dendritic cells. Glycobiology **2004**; 14:647–57.
21. Coelho PS, Klein A, Talvani A, et al. Glycosylphosphatidylinositol-anchored mucin-like glycoproteins isolated from *Trypanosoma cruzi* trypomastigotes induce in vivo leukocyte recruitment dependent on MCP-1 production by IFN-gamma-primed-macrophages. J Leukoc Biol **2002**; 71:837–44.
22. Schmitz V, Svensjo E, Serra RR, Teixeira MM, Scharfstein J. Proteolytic generation of kinins in tissues infected by *Trypanosoma cruzi* depends on CXC chemokine secretion by macrophages activated via Toll-like 2 receptors. J Leukoc Biol **2009**; 85:1005–14.
23. Kleshchenko YY, Moody TN, Furtak VA, Ochieng J, Lima MF, Villalta F. Human galectin-3 promotes *Trypanosoma cruzi* adhesion to human coronary artery smooth muscle cells. Infect Immun **2004**; 72:6717–21.
24. Moody TN, Ochieng J, Villalta F. Novel mechanism that *Trypanosoma cruzi* uses to adhere to the extracellular matrix mediated by human galectin-3. FEBS Lett **2000**; 470:305–8.
25. Castellani O, Ribeiro LV, Fernandes JF. Differentiation of *Trypanosoma cruzi* in culture. J Protozool **1967**; 14:447–51.
26. Council directive from the Convention for the Protection of Vertebrate Animals Used for Experimental and Other Scientific Purposes (Strasbourg, France). 18 March 1986.
27. Piron M, Fisa R, Casamitjana N, et al. Development of a real-time PCR assay for *Trypanosoma cruzi* detection in blood samples. Acta Trop **2007**; 103:195–200.
28. Pineda MA, Corvo L, Soto M, Escudero MF, Bonay P. Interactions of human galectins with *Trypanosoma cruzi*. Glycobiology **2015**; 25: 197–210.
29. Joffre O, Nolte MA, Sporri R, Reis e Sousa C. Inflammatory signals in dendritic cell activation and the induction of adaptive immunity. Immunol Rev **2009**; 227:234–47.
30. Oliveira AC, de Alencar BC, Tzelepis F, et al. Impaired innate immunity in Tlr4(-/-) mice but preserved CD8+ T cell responses against *Trypanosoma cruzi* in Tlr4-, Tlr2-, Tlr9- or Myd88-deficient mice. PLoS Pathog **2010**; 6:e1000870.
31. Koga R, Hamano S, Kuwata H, et al. TLR-dependent induction of IFN-beta mediates host defense against *Trypanosoma cruzi*. J Immunol **2006**; 177:7059–66.
32. Campos MA, Almeida IC, Takeuchi O, et al. Activation of Toll-like receptor-2 by glycosylphosphatidylinositol anchors from a protozoan parasite. J Immunol **2001**; 167:416–23.
33. Gravina HD, Antonelli L, Gazzinelli RT, Ropert C. Differential use of TLR2 and TLR9 in the regulation of immune responses during the infection with *Trypanosoma cruzi*. PLoS One **2013**; 8:e63100.
34. Tellez-Sanz R, Garcia-Fuentes L, Vargas-Berenguel A. Human galectin-3 selective and high affinity inhibitors. Present state and future perspectives. Curr Med Chem **2013**; 20:2979–90.
35. Karayannis G, Triposkiadis F, Skoularigis J, Georgoulias P, Butler J, Giamouzis G. The emerging role of Galectin-3 and ST2 in heart failure: practical considerations and pitfalls using novel biomarkers. Curr Heart Fail Rep **2013**; 10:441–9.
36. Henderson NC, Sethi T. The regulation of inflammation by galectin-3. Immunol Rev **2009**; 230:160–71.
37. Soares MB, Lima RS, Souza BS, et al. Reversion of gene expression alterations in hearts of mice with chronic chagasic cardiomyopathy after transplantation of bone marrow cells. Cell Cycle **2011**; 10:1448–55.
38. Toscano MA, Bianco GA, Ilarregui JM, et al. Differential glycosylation of TH1, TH2 and TH-17 effector cells selectively regulates susceptibility to cell death. Nat Immunol **2007**; 8:825–34.
39. Demetriou M, Granovsky M, Quaggin S, Dennis JW. Negative regulation of T-cell activation and autoimmunity by Mgat5 N-glycosylation. Nature **2001**; 409:733–9.
40. Joo HG, Goedegebuure PS, Sadanaga N, Nagoshi M, von Bernstorff W, Eberlein TJ. Expression and function of galectin-3, a beta-galactoside-binding protein in activated T lymphocytes. J Leukoc Biol **2001**; 69:555–64.
41. Sharma U, Rhaleb NE, Pokharel S, et al. Novel anti-inflammatory mechanisms of N-Acetyl-Ser-Asp-Lys-Pro in hypertension-induced target organ damage. Am J Physiol Heart Circ Physiol **2008**; 294: H1226–32.
42. Sharma UC, Pokharel S, van Brakel TJ, et al. Galectin-3 marks activated macrophages in failure-prone hypertrophied hearts and contributes to cardiac dysfunction. Circulation **2004**; 110:3121–8.
43. de Boer RA, Voors AA, Muntendam P, van Gilst WH, van Veldhuisen DJ. Galectin-3: a novel mediator of heart failure development and progression. Eur J Heart Fail **2009**; 11:811–7.
44. Yu L, Ruifrok WP, Meissner M, et al. Genetic and pharmacological inhibition of galectin-3 prevents cardiac remodeling by interfering with myocardial fibrogenesis. Circ Heart Fail **2013**; 6:107–17.
45. Petersen CA, Krumholz KA, Burleigh BA. Toll-like receptor 2 regulates interleukin-1beta-dependent cardiomyocyte hypertrophy triggered by *Trypanosoma cruzi*. Infect Immun **2005**; 73:6974–80.
46. Amith SR, Jayanth P, Franchuk S, et al. Neu1 desialylation of sialyl alpha-2,3-linked beta-galactosyl residues of TOLL-like receptor 4 is essential for receptor activation and cellular signaling. Cell Signal **2010**; 22:314–24.
47. Ozinsky A, Underhill DM, Fontenot JD, et al. The repertoire for pattern recognition of pathogens by the innate immune system is defined by cooperation between toll-like receptors. Proc Natl Acad Sci U S A **2000**; 97:13766–71.
48. Ropert C, Gazzinelli RT. Regulatory role of Toll-like receptor 2 during infection with *Trypanosoma cruzi*. J Endotoxin Res **2004**; 10:425–30.
49. Ouaissi A, Guilvard E, Delneste Y, et al. The *Trypanosoma cruzi* Tc52-released protein induces human dendritic cell maturation, signals via Toll-like receptor 2, and confers protection against lethal infection. J Immunol **2002**; 168:6366–74.
50. Hirata N, Yanagawa Y, Ebihara T, et al. Selective synergy in anti-inflammatory cytokine production upon cooperated signaling via TLR4 and TLR2 in murine conventional dendritic cells. Mol Immunol **2008**; 45:2734–42.